Special Supplement: Climate Change in Agriculture

Optimal soybean sowing window adjusted to climatic variability based on El Niño-Southern Oscillation using agrometeorological modeling[1]

Marcus José Alves de Lima[2], Hildo Giuseppe Garcia Caldas Nunes[2], Leila Sobral Sampaio[2], Paulo Jorge de Oliveira Ponte de Souza[2], Clyde William Fraisse[3]

ABSTRACT

Determining the optimal sowing window (OSW) based on climate variability associated with El Niño-Southern Oscillation (ENSO) can provide valuable information for agricultural planning in the tropics. This study aimed to calibrate, evaluate and apply the CROPGRO-Soybean model for determining the OSW across the ENSO phases for soybean-producing areas in the Pará State, northern Brazil. First, the model was calibrated and evaluated using experimental data collected in the field, between 2006 and 2009. In this process, the model estimates showed a good agreement with the observed data for soybean phenology, growth and yield, demonstrating potential to simulate the crop yield in this part of the Amazon. After calibration, the model was used in the seasonal mode to simulate 18 planting dates, over 39 years and in three locations. The simulated yields were divided into three ENSO phases. The set of sowing dates that showed a high frequency (> 80 %) of yields above 3,500 kg ha^{-1} integrated the OSW for each location and ENSO phases. The OSW duration differed between locations and ENSO phases, varying more during La Niña than El Niño events. However, regardless of the location or ENSO phase, late sowing was more suitable, because, besides favoring a greater frequency of good climate conditions for the development, growth and high yields, it also favors a lower risk of rainfall during the harvest period.

KEYWORDS: *Glycine max*, CROPGRO-Soybean model, climate risk mitigation.

RESUMO

Janela ótima de semeadura da soja ajustada à variabilidade climática baseada em El Niño-Oscilação Sul utilizando-se modelagem agrometeorológica

A determinação da janela ótima de semeadura (JOS), de acordo com a variabilidade climática associada ao El Niño-Oscilação Sul (ENOS), pode fornecer informações valiosas para o planejamento agrícola nos trópicos. Objetivou-se calibrar, avaliar e aplicar o modelo CROPGRO-Soybean na determinação da JOS nas fases de ENOS para áreas produtoras de soja no estado do Pará. Primeiramente, o modelo foi calibrado e avaliado a partir de dados experimentais coletados em campo, entre 2006 e 2009. Nesse processo, as estimativas do modelo mostraram boa concordância com os dados observados para fenologia, crescimento e produtividade da soja, demonstrando potencial para simular o rendimento da cultura nessa parte da Amazônia. Após a calibração, o modelo foi utilizado no modo sazonal, para simular 18 datas de semeadura, em 33 anos e três locais. Os rendimentos simulados foram separados de acordo com três fases ENOS. O conjunto de datas de semeadura que apresentou alta frequência (> 80 %) de rendimentos acima de 3.500 kg ha^{-1} integrou a JOS para cada local e fase ENOS. A duração da JOS foi diferente entre os locais e fases ENOS, variando mais durante eventos de La Niña do que de El Niño. No entanto, independentemente do local ou da fase ENOS, a semeadura tardia foi mais indicada, pois, além de favorecer uma maior frequência de boas condições climáticas para o desenvolvimento, crescimento e altas produtividades, também favorece um menor risco de chuvas durante o período de colheita.

PALAVRAS-CHAVES: *Glycine max*, modelo CROPGRO-Soybean, mitigação de riscos climáticos.

INTRODUCTION

Rainfed agriculture is probably the most weather-dependent economic activity (Ray et al. 2015). However, in low-latitude regions, where photoperiod, temperature, humidity and solar radiation have low variability, rainfall is the greatest source of risk to crop yield (Lima et al. 2019), especially in the Amazon, where the vast majority of the agriculture production is under rainfed conditions, and the rainfall pattern is strongly modified by the El Niño-Southern Oscillation (ENSO) phenomenon (Sousa et al. 2015).

ENSO is a large-scale phenomenon that alters the weather patterns of several places worldwide,

[1] Received: Mar. 30, 2022. Accepted: May 26, 2022. Published: July 13, 2022. DOI: 10.1590/1983-40632022v5272428.
[2] Universidade Federal Rural da Amazônia, Belém, PA, Brasil.
E-mail/ORCID: marcus.lima@ufra.edu.br/0000-0002-6207-6284; garibalde13@gmail.com/0000-0003-4072-003X; lsobralsampaio@gmail.com/0000-0003-0685-1757; paulo.jorge@ufra.edu.br/ 0000-0003-4748-1502.
[3] University of Florida, Gainesville, FL, United States of America. *E-mail/ORCID*: cfraisse@ufl.edu/0000-0001-9875-2187.

causing serious problems for agriculture depending on its phase (El Niño or La Niña) and intensity. In the Amazon, El Niño events are generally associated with intense droughts, whereas La Niña events are associated with heavy rainfall and abnormal floods (Shimizu et al. 2017). The ENSO impacts on the Amazon climate, in terms of ecology and hydrology, are well documented (Shimizu et al. 2017, Brum et al. 2018). However, studies about the ENSO effects on agricultural yield in the region are scarce, even with agricultural losses often evidenced in El Niño years, such as the reduction in soybean yields in the States of northern Brazil in 2015 and 2016 (Nóia Júnior & Sentelhas 2019)

One of the methods to minimize the negative effects of climate on the soybean crop is changing the planting date, thus exposing the crop cycle to meteorological conditions favorable to high yields (Lima et al. 2019). In the present study, it is hypothesized that the optimal sowing window (OSW) may change according to the ENSO phase (El Niño, La Niña and neutral). This hypothesis has been previously tested and confirmed through simulations using dynamic crop models that integrate meteorological elements, soil characteristics and crop management (Hallinor et al. 2018, Lima et al. 2019, Nóia Júnior & Sentelhas 2019), and these studies emphasize the potential of crop models as a tool for climate risk analysis.

In this context, the CROPGRO-Soybean model stands out, as it was developed to simulate the main physical and physiological processes of soybean growth based on daily weather conditions, physical and chemical soil characteristics, crop management and genetic characteristics of the cultivar (Boote et al. 2001), and has been widely used in several tropical environments to assess the effects of climate or crop management on soybean yields (Nóia Júnior & Sentelhas 2019, Reis et al. 2020, Silva et al. 2021).

Thus, this study aimed to calibrate, evaluate and apply the CROPGRO-Soybean model to investigate the effects of the ENSO phases on soybean yield in the Amazon, as well as to define the OSW, as a strategy to mitigate the climatic risks of the ENSO phases.

MATERIAL AND METHODS

The study was carried out in Paragominas (3º05'S; 47º20'W), Santarém (2º38'S; 54º57'W) and Conceição do Araguaia (8º16'S; 49º16'W) (all in the Pará State, Brazil), due to their relevance in the soybean production (IBGE 2017) and for having a long series of climatic data. To create the climate files required by the CROPGRO-Soybean model, long-term daily records (1981-2019) of the maximum and minimum air temperature values, sunshine hours and rainfall were obtained from the Brazilian national meteorology institute (INMET) (Brasil 2022). The solar radiation values for the three locations were estimated as a function of sunshine hours using the equation given by Angstrom-Prescott, with monthly coefficients adjusted to the Amapá State, northern Brazil (Belúcio et al. 2014).

In the case of Paragominas, since the INMET weather station was recently installed (2006), it was necessary to group the weather data from other sources to equate the number of years in the climatological series used for the other two locations. For example, the rainfall data were obtained from the Brazilian water agency (Brasil 2022) and the maximum and minimum air temperature data and sunshine hours from the Empresa Brasileira de Pesquisa Agropecuária (Embrapa 2022). Missing values for temperature (maximum and minimum) and sunshine hours were obtained from the nearest weather stations within a radius of 200 km (Bier & Ferraz 2017).

The soil characterization data used in the simulations were obtained from previous studies on natural resources in the Pará State, documented in exploratory maps of Brazilian soils and published by the Radam Brasil Project (1973-1974) (Brasil 1974). These studies provided the physical and chemical characteristics of the soil in layers up to 1-m deep. The soil water contents at field capacity and permanent wilting point for each soil layer were estimated using the Van Genuchten equations [$\theta s = 1 + (-0.00037 \times Bd)$ and $\theta r = 0.0858 - (0.1671 \times \text{sand}) + 0.3516 \times \text{clay} + 1.1846 \times \text{OC} + 0.000029 \times Bd$, where θs and θr represent the soil water content at field capacity and permanent wilting point ($m^3\ m^{-3}$), respectively, OC is the organic carbon content ($g\ kg^{-1}$) and *Bd* the soil density ($Mg\ m^{-3}$)], with parameters adjusted for tropical soil (Medeiros et al. 2014). Table 1 presents the physical characteristics and pH of the topsoil (0-20 cm) of the studied locations.

Experimental data collected from a commercial production farm in Paragominas were used for model calibration and evaluation. Data from two crop

Table 1. Topsoil (0-20 cm) data from three series that are representative for soybean producing regions in the Pará State, Brazil.

Municipality	Bulk density	Sand	Clay	Silt	pH	Source: Radam Brasil project (1973-1974)
	Mg m^{-3}		g kg^{-1}			
Paragominas	1.27	190	780	30	5.7	Index map SA.22/SA.23
Santarém	1.22	100	820	80	4.5	Index map SA.21
Conceição do Araguaia	2.25	210	440	350	6.1	Index map SB.22

seasons (2006 and 2008) were used to calibrate the model. Similar management practices were used in both campaigns: row spacing of 0.5 m, planting density of 22 plants m^{-2} and fixed-growth BRS-Tracajá cultivar, maturity group 9.2. The seeds were previously treated with *Rhizobium* inoculant, fungicides and insecticides. During the sowing period, the soil was fertilized with 640 kg ha^{-1} of NPK (2:20:28). The crop phenology was observed daily using the growth staging method by Fehr & Caviness (1977). Starting at ten days after planting, destructive samples with area of 0.5 m^2 (six replications) were randomly taken throughout the growing season, at intervals of 10-20 days. On each sampling date, the plants were dried in a forced-air oven at 70 ºC, until constant weight, and then partitioned to determine the leaf, stem, pod and grain weight. The leaf area index was determined using the leaf disk method, at the physiological maturity, and six replications with area of 1 m^2 each were sampled to determine the average yield and harvest index (Souza et al. 2011).

For model validation, the yield data of trials conducted in 2007 and 2009 were used, with the same cultivar used for calibration under different planting dates: Feb. 23, 2007 (22 plants m^{-2}) and Jan. 17, 2009 (22 plants m^{-2}), as well as a more complete experiment with two planting dates (Feb. 24 and Mar. 14) and four planting densities (10, 20, 30 and 40 plants m^2) of the BRS-Sambaíba cultivar - a conventional cultivar with characteristics (maturity group and crop cycle) similar to the cultivar used in the calibration process (BRS-Tracajá).

The CROPGRO-Soybean calibration process was used to determine a combination of genetic coefficients of cultivars, with values within realistic ranges that minimize model errors. The genetic coefficients were estimated based on the observed date of the main phenological phases (first flowering, first pod, first seed and physiological maturity), growth curves of leaf, stem and pod biomass, leaf area index and grain yield of the BRS-Tracajá soybean cultivar. A generic cultivar of the maturity group nine was used to start the calibration process. An iterative approach of trial-and-error adjustments was carried out until there was a reasonable match between the observed and simulated values, starting with the parameters for phenology and followed by the crop growth parameters (Boote et al. 2001).

The accuracy of the genetic coefficients was determined by comparing the simulated values of development and growth with their corresponding observed values, using the normalized root mean square error: $nRMSE = \sqrt{[\sum_{i=1}^{n} (y_i - \hat{y}_i)^2 / n]} \times (100/\bar{y})$; the index of agreement: $d = 1 - [\sum_{i=1}^{n} (y_i - \hat{y}_i)^2 / \sum_{i=1}^{n} (|\hat{y}_i - \bar{y}| + |y_i - \bar{y}|)^2]$; and modeling efficiency: $ME = 1 - \sum_{i=1}^{n}$, where n is the total number of observations, y and $\hat{y}$ the observed and predicted values, respectively, and $\bar{y}$ the overall mean of the observed values. The model performance was evaluated by comparing the simulated yield with an independent data set obtained experimentally under different growth conditions (Wallach et al. 2014).

The rainfed soybean yield was simulated for each studied location using the calibrated model in the seasonal cropping module of the DSSAT 4.6 software. The simulations were performed for the 1st and 15th days of each month, starting in September and ending in May, resulting in 18 planting dates, 3 counties and 39 years, totaling 2,106 simulations. Once yields were simulated for each location, considering the planting density of 22 plant m^{-2}, the results were split into three ENSO phases using the Oceanic Niño Index (ONI) as an indicator (USA 2017).

The optimal sowing window was then determined by subgrouping the planting dates with at least an 80 % probability of simulating high yields. Considering that the average soybean yield in the main Brazilian producing States has oscillated between 2,756 and 3,393 kg ha^{-1} (Sentelhas et al. 2015), this study considered yields > 3,500 kg ha^{-1} as a higher yield threshold.

RESULTS AND DISCUSSION

Half of the 18 cultivar coefficients that express the development and growth of soybean in the CROPGRO-Soybean model were modified, in addition to two ecotype coefficients. The cultivar coefficients with higher contrasts in relation to the generic cultivar were: time between plant emergence and flower appearance and time between the first seed appearance and physiological maturity. The ecotype coefficients expressing the time from the appearance of the first flower to the last leaf on the main stem and the rate of appearance of leaves on the main stem were slightly increased to reproduce the leaf production characteristics of the BRS-Tracajá cultivar (Table 2). Except for the slope of the relative development response to photoperiod with time and time between plant emergence and flower appearance, all the other cultivar coefficients were within the range reported by Boote et al. (2001).

The graphical analysis showed a "good" agreement to most the observed points throughout the growth season (Figure 1). The observed disparities for top biomass and leaf area index from 70 to 105 days after planting (Figures 1A-C) may have been caused by leaf retention, a physiological disorder not accounted for by the model. Leaf retention favors the maintenance of green leaves and stem, what is very common in rainy years with excessive rainfall during the maturation period, similarly to that described by Holshouser (2009). However, no major disagreement was found between the simulated pod biomass curve and the respective observed curve from both trials (Figures 1A and 1B), indicating that leaves retained due to the physiological disorder seem to have no biomass translocation activity to seed and, thus, no effect on the simulated yield.

The model validation was carried out using soybean yield data obtained from independent experiments carried out in Paragominas. Simulated yields ranged from 2,738 to 4,065 kg ha^{-1}, and observed yields from 2,587 to 4,040 kg ha^{-1}. The difference between simulated and observed yields was lower than 5 %, indicating a slight overestimation. The graphical analysis also showed that the model tends to overestimate yield for most growing conditions, but the deviation was within a ±15 % range in all cases (Figure 2), which is generally acceptable in crop simulation studies (Vilayvong et al. 2015). In general, the model performed satisfactorily and could explain 69 % (EF = 0.69) of the observed variability from different management practices.

Considering the average monthly rainfall in Paragominas, Santarém and Conceição do Araguaia for the different ENSO phases, it was evident that in neutral years it was quite similar to those observed in normal years (average of all years). The largest differences in the average monthly rainfall were observed when either El Niño or La Niña occurred (Figure 3). For example, in Paragominas, during El Niño years, the values ranged from 13 to 41 % below normal during the whole rainy season, while, in La Niña years, they ranged from 24 to 85 % above normal during November, December, March, April and May (Figure 3A).

Table 2. Cultivar coefficients for the soybean maturity group nine (generic coefficients from the DSSAT software) and the BRS-Tracajá soybean cultivar (used in the calibration process).

Cultivar trait	Unit	Generic cultivar	BRS-Tracajá
1. Critical short-day length below which reproductive development progresses without the effect of day length	h	11.880	11.600
2. Slope of the relative developmental response to photoperiod with time	h^{-1}	0.340	0.355
3. Time between plant emergence and flower appearance (R1)	Pd	23.000	30.500
4. Time between first flower and first pod appearance (R3)	Pd	10.000	9.000
5. Time between first flower and first seed appearance (R5)	Pd	16.000	14.000
6. Time between first seed appearance (R5) and physiological maturity (R7)	Pd	37.400	30.000
7. Duration of seed filling for pod cohort under standard growth conditions	Pd	23.000	20.500
8. Specific leaf area of the cultivar under standard growth conditions	cm^2 g^{-1}	375.000	350.000
9. Maximum size of a full leaf (three leaflets)	cm^2	180.000	200.000
Ecotype trait			
1. Time from the appearance of the first flower to the last leaf on the main stem	Pd	9.000	12.000
2. Rate of leaf appearance on the main stem	Pd	0.320	0.380

Pd: photothermal day.

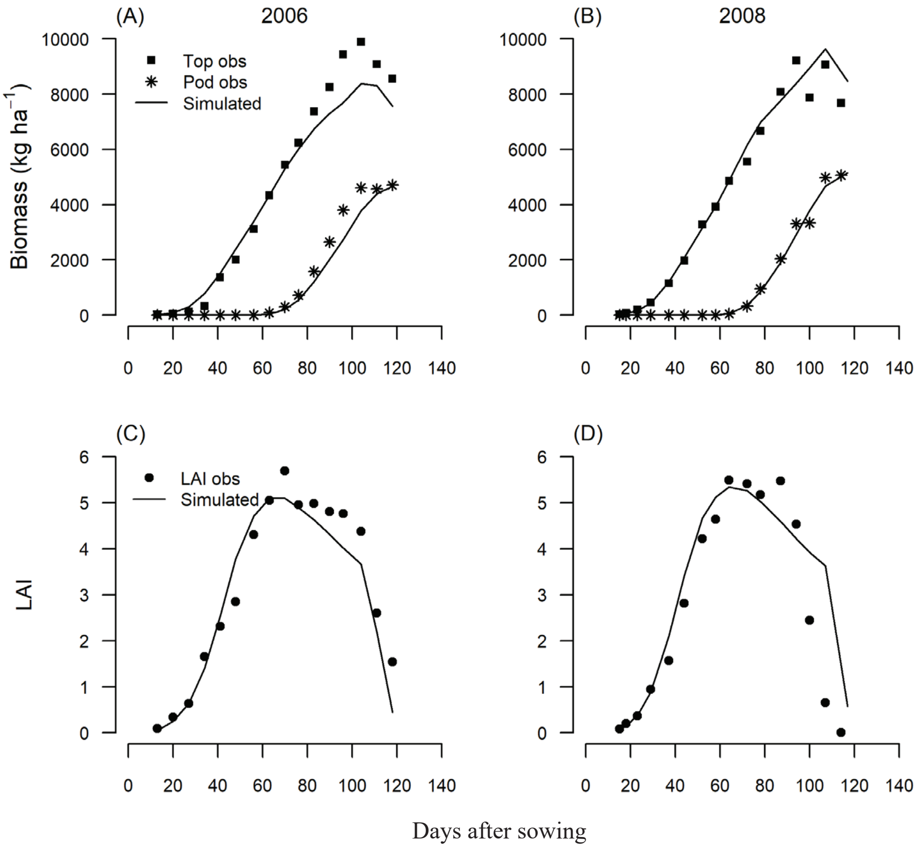

Figure 1. Comparison between simulated and observed (obs) values for top and pod biomass and leaf area index (LAI) for the BRS-Tracajá cultivar, in 2006 (A and C) and 2008 (B and D), following the model calibration.

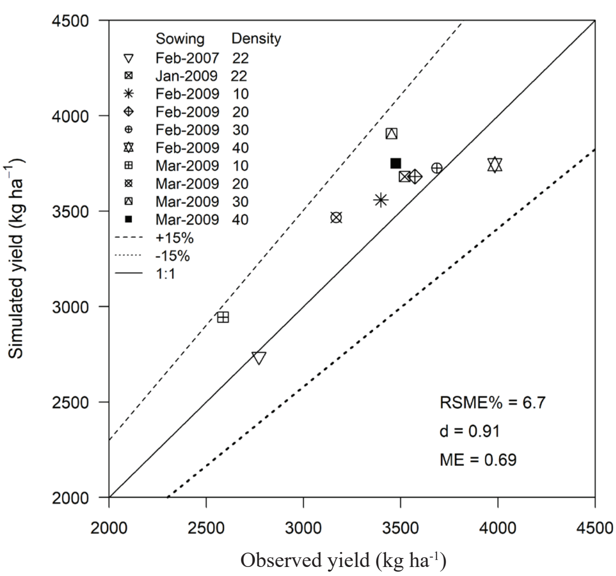

Figure 2. Comparison between simulated and observed values for yield of the BRS-Tracajá soybean cultivar, under different crop managements (planting and density dates), for model evaluation. RMSE%: normalized root mean square error; d: index of agreement; ME: modeling efficiency.

The average monthly rainfall pattern in Santarém differed from that in Paragominas, where the volume deviation across the ENSO phases was evident only in the three first months of the year. During El Niño years, in January, it was, on average, 123 mm (59 % lower than normal). This difference decreased to near zero in April and remained this way until the next austral summer. A similar trend was observed during the La Niña years, but ranging from 29 to 46 % above normal during the same period (Figure 3B). The pattern in Conceição do Araguaia also differed from that in the other two sites. For example, large deviations were not observed during the La Niña years, except in November, when the volume was 35 % above normal. In contrast, during the El Niño years, it ranged from 1 to 37 % below normal during the rainy season, being lower during February (Figure 3C).

These results demonstrated that the ENSO effects differ for each location, being more intense in Paragominas than in Santarém and Conceição do Araguaia. Indeed, during the El Niño (or La Niña)

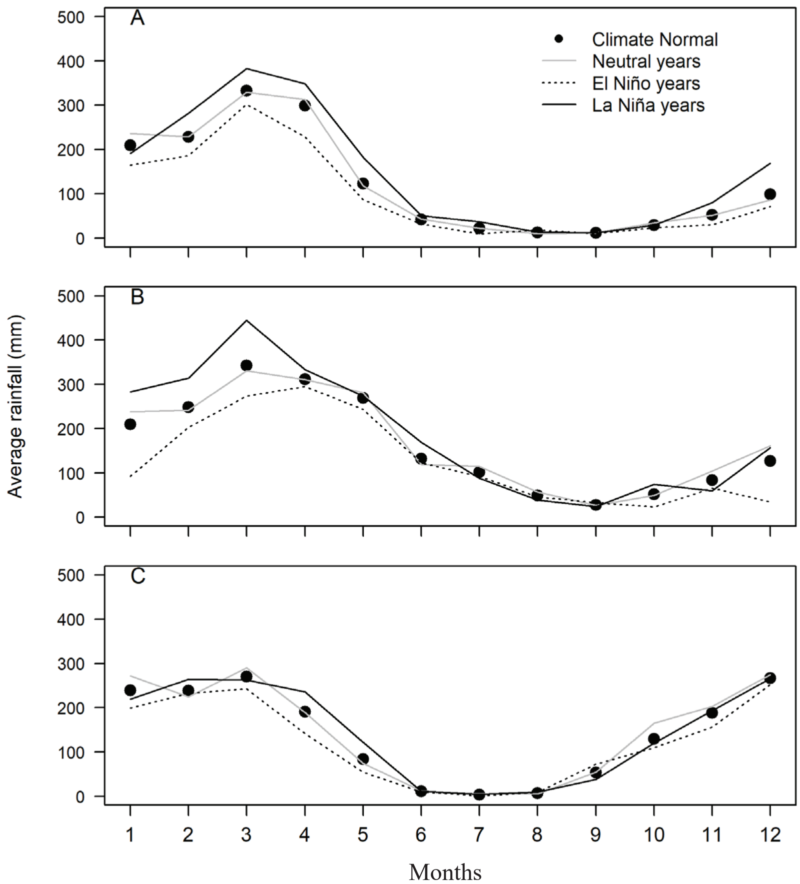

Figure 3. Average monthly rainfall in Paragominas (A), Santarém (B) and Conceição do Araguaia (C) across the El Niño-Southern Oscillation phases and for the average of all years. Note: the averages obtained from historical weather data (1981-2019) were 10 El Niño years, 11 La Niña years and 18 neutral years.

years, the Amazon experiences negative (or positive) rainfall anomalies in almost its whole area. However, this relationship plays a more important role during the rainy season (summer and austral fall), when higher values of rainfall anomalies are usually observed in the central, northern and northeastern parts of Brazil (Sousa et al. 2015).

The simulation results indicated that the OSW length differed for each location and across the ENSO phases. For example, in Paragominas, it decreased from 75 days (Dec. 1 - Feb. 15) in neutral years to 45 days (Dec. 15 - Feb. 1) in El Niño years and extended to 120 days (Nov. 1 - Mar. 1) in La Niña years. This variation pattern suggests that the planting dates from Nov. 1 to Dec. 1 and from Feb. 15 to Mar. 1 represent important and strategic periods to be considered for minimizing the effects of extreme ENSO events. The OSW center period (Dec. 15 - Feb. 1) does not undergo the ENSO influence (Figures 4A, 4D and 4G). Choosing a sowing date that shifts the growing season may expose the crop to water stress or good weather conditions. A detailed analysis of how the choice of sowing date affects soybean yield in the Amazonian production environment is seen in a study by Lima et al. (2019).

The OSW length variability in Santarém during El Niño and La Niña years showed a similar trend in relation to Paragominas, but with a different pattern. The OSW length in Paragominas ranged from center to the extremities of the suitable window, whereas this variation was more evident for the early planting dates in Santarém. During the neutral years, the high yield probabilities for the planting dates Nov. 15, Dec. 1 and Dec. 15 were, respectively, 74, 79 and 95 %; however, these probabilities decreased to 25, 25 and 62 %, respectively, during El Niño events and increased to 95 % for the three planting dates during La Niña events (Figures 4B, 4E and 4H). In summary, the period between Nov. 15 and Dec. 15 also

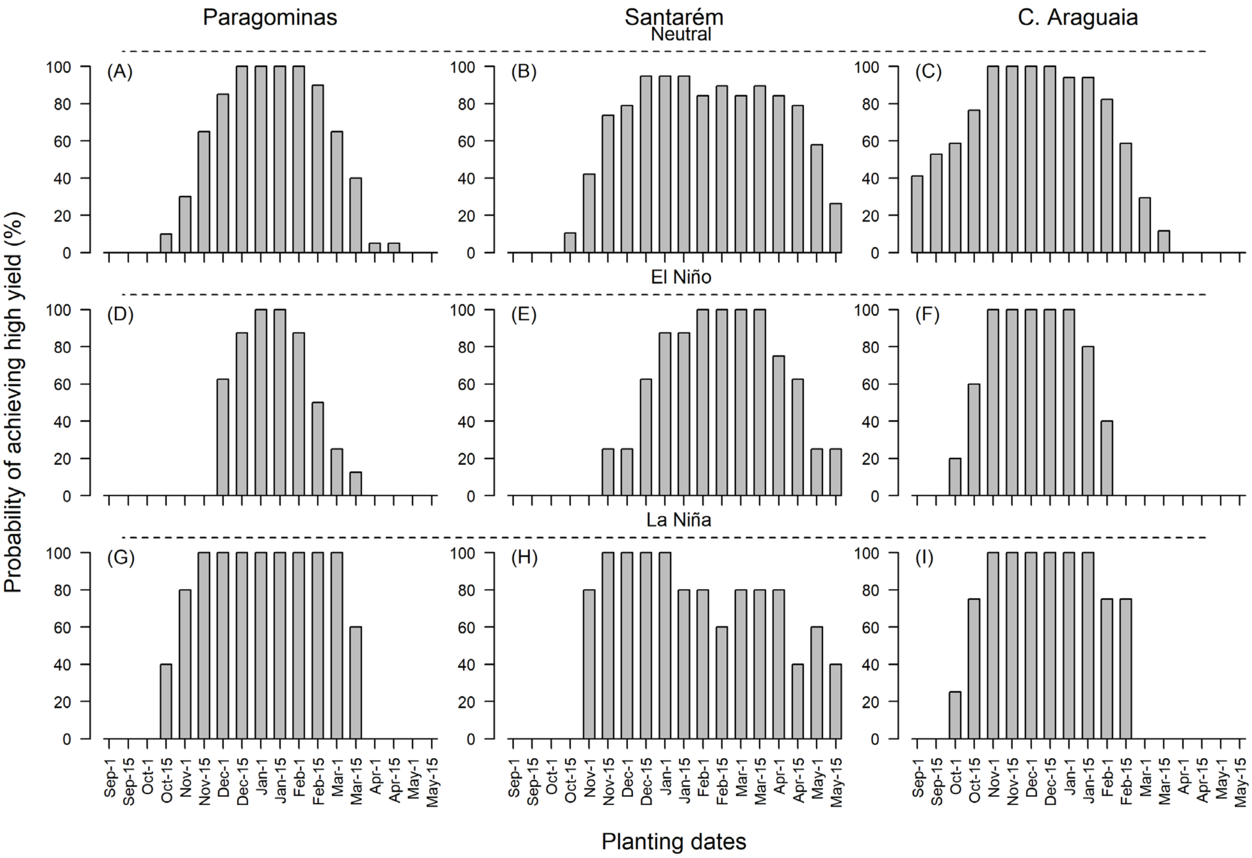

Figure 4. Probabilities for a high yield (> 3,500 kg ha^{-1}) of soybean at different planting dates in Paragominas (A, D and G), Santarém (B, E and H) and Conceição do Araguaia (C, F and I), across the ENSO phases. Note: number of simulated crop seasons: 18 neutral years, 10 El Niño years and 11 La Niña years (1981-2019).

represents a strategic period for agricultural planning in the face of a predicted ENSO phenomenon.

Conceição do Araguaia showed a low variability in OSW length across the ENSO phases (75-90 days). No difference was found in the OSW length between El Niño and La Niña events (Figures 4C, 4F and 4I), although there was a reduction in the average monthly rainfall from 2 to 37 % during El Niño years (Figure 1C). The high soil clay content (44 %) probably influenced this result. Woli et al. (2013) analyzed the ENSO effects on peanut yield under different soil types in southeastern USA and concluded that only light-textured or coarse soils with low water-holding capacities resulted in significant yield differences. The ENSO did not significantly influence medium or heavy soils, because they can hold water for a longer period and maintain adequate soil moisture levels to sustain plant growth even under high rainfall variability.

Although Paragominas and Santarém are in the same climatic zone (Am) of the Köppen's climate classification (Alvares et al. 2013), the ENSO seems to affect them differently. According to Paz et al. (2012), interactions between physiographic factors, such as the presence of large forests and/or large water bodies, and the regional climate can buffer the ENSO effect. Other studies have also reported that large areas of the Amazon basin are sensitive to the effects of deforestation (Nobre et al. 2009). They agree that the forest accounts for a considerable portion of the regional water budget.

The vulnerability of soybean yields to extreme ENSO effects was higher in Paragominas than in the other two studied sites, because, unlike Santarém and Conceição do Araguaia, Paragominas is not close to large water bodies, what may have influenced this result, because regions where physiographic features are not evident or strong enough to create a microclimate are more likely to experience significant ENSO effects (Woli et al. 2013). For these locations, the OSW determined by the agricultural zoning of climate risk may be flawed, because its simplified methodology is not sensitive to high anomalies of the climatological normal observed in El Niño or La Niña years (Nóia Júnior & Sentelhas 2019).

The agricultural zoning of climate risk for the Pará State in the 2019/2020 harvest plan (Brasil 2019) presented a OSW of 52 days (Dec. 10 - Jan. 31) for Paragominas, 61 days (Dec. 1 - Jan. 31) for Santarém and 113 days (Oct. 10 - Jan. 31) for Conceição do Araguaia. Comparing these results with those obtained in this study, a good similarity was observed for neutral years, given that the results were practically contained in the OSW determined by the CROPGRO-Soybean model, indicating that the simplified agricultural zoning of climate risk methodology was efficient, especially for places with a low influence of the ENSO, such as Conceição do Araguaia. On the other hand, the use of the CROPGRO-Soybean model is more effective in places with climate variabilities due to the ENSO, such as Paragominas and Santarém.

Several researchers have investigated the ENSO effects on simulated yields of important economic crops, such as peanut, cotton, corn and soybean, in different locations and planting dates (Paz et al. 2012, Waongo et al. 2015, Woli et al. 2015), and concluded that the planting dates that favored a higher yield and a lower variation coefficient varied across locations and ENSO phases. These studies have demonstrated that the risk of crop production at a given location depends on the planting date and the current ENSO phase. This approach can accelerate the production of technological information, with results that may help policymakers and farmers to prepare for future threats of climate variability and change, which are likely to increase in intensity and frequency (Bilali et al. 2020).

CONCLUSIONS

1. The CROPGRO model satisfactorily simulated the growth and development of soybean under the soil and climate conditions of the Amazon. The model was also sensitive to rainfall variations caused by the El Niño-Southern Oscillation (ENSO) phase, as it coherently simulated an optimal sowing window for high yields and improved the understanding of soybean yield risks associated with ENSO-based climate variability in the area;
2. The hypothesis tested in this study was partially accepted, as the optimal sowing window for Conceição do Araguaia remained unchanged between ENSO phases, whereas it shifted explicitly for Paragominas and Santarém.

ACKNOWLEDGMENTS

The authors thank the Fundação Amazônia de Amparo a Estudos e Pesquisas (Fapespa), Conselho Nacional de Desenvolvimento Científico e Tecnológico (CNPq) and Coordenação de Aperfeiçoamento de Pessoal de Nível Superior (Capes).

REFERENCES

ALVARES, C. A.; STAPE, J. L.; SENTELHAS, P. C.; MORAES, G. J. L.; SPAROVEK, G. Köppen's climate classification map for Brazil. *Meteorologische Zeitschrift*, v. 22, n. 6, p. 711-728, 2013.

BELÚCIO, L. P.; SILVA, A. P. N.; SOUZA, L. R.; MOURA, G. B. A. Radiação solar global estimada a partir da insolação para Macapá (AP). *Revista Brasileira de Meteorologia*, v. 29, n. 4, p. 494-504, 2014.

BIER, A. A.; FERRAZ, S. E. T. Comparação de metodologias de preenchimentos de falhas em dados meteorológicos para estações no sul do Brasil. *Revista Brasileira de Meteorologia*, v. 32, n. 2, p. 215-226, 2017.

BILALI, H.; BASSOLE, I. H. N.; DAMBO, L.; BERJAN, S. Climate change and security. *Agriculture and Forestry*, v. 66, n. 3, p. 197-210, 2020.

BOOTE, K. J.; KROPFF, M. J.; BINDRABAN, P. S. Physiology and modelling of traits in crop plants: implications for genetic improvement. *Agricultural Systems*, v. 70, n. 2, p. 395-420, 2001.

BRASIL. Agência Nacional das Águas (ANA). *Hidroweb*: séries históricas de estações. 2022. Available at: https://www.snirh.gov.br/hidroweb/serieshistoricas. Access on: Jan. 05, 2022.

BRASIL. Instituto Nacional de Meteorologia (Inmet). *Banco de dados meteorológicos do Inmet*. 2022. Available at: https://bdmep.inmet.gov.br/#. Access on: Jan. 10, 2022.

BRASIL. Departamento Nacional de Produção Mineral. *Projeto Radam*: levantamento de recursos naturais. 1974. Available at: biblioteca.ibge.gov.br. Access on: Mar. 27, 2022.

BRASIL. Portaria n. 69, de 11 de junho de 2019. Aprova o zoneamento agrícola de risco climático para a cultura de soja no estado do Pará, ano-safra 2019/2020. *Diário Oficial da União*, seção 1, Brasília, DF, p. 55, 12 abr. 2019.

BRUM, M.; LÓPEZ, J. G.; ASBJORNSEN, H.; LICATA, J.; PYPKER, T.; SANCHEZ, G.; OLIVEIRA, R. S. ENSO effects on the transpiration of eastern Amazon trees. *Philosophical Transactions of the Royal Society B: Biological Sciences*, v. 373, e1760, 2018.

EMPRESA BRASILEIRA DE PESQUISA AGROPECUIÁRIA (Embrapa). *Agritempo*. 2022. Available at: https://www.agritempo.gov.br/agritempo/jsp/PesquisaClima/index.jsp?siglaUF=PA. Access on: Jan. 02, 2022.

FEHR, W. R.; CAVINESS, C. E. *Stages of soybean development*. Ames: Iowa State University, 1977.

HALLINOR, A. J.; MÜLLER, C.; ASSENG, S.; DEVA, C.; NICKLIN, K. J.; WALLACH, D.; VANUYTRECHT, E.; WHITFIELD, S.; RAMIREZ-VILLEGAS, J.; KOEHLER, A. Improving the use of crop models for risk assessment and climate change adaptation. *Agricultural Systems*, v. 159, n. 1, p. 269-306, 2018.

HOLSHOUSER, D. *Green stem syndrome in soybean*. 2009. Available at: www.ext.vt.edu. Access on: Mar. 27, 2022.

INSTITUTO BRASILEIRO DE GEOGRAFIA E ESTATÍSTICA (IBGE). *Levantamento sistemático da produção agrícola*. 2017. Available at: https://www.ibge.gov.br/estatisticas/economicas/agricultura-e-pecuaria. Access on: Feb. 20, 2022.

LIMA, M. J. A.; OLIVEIRA, E. C.; SAMPAIO, L. S.; FRAISSE, C. W.; SOUZA, P. J. O. P. Agrometeorological analysis of the soybean potentiality in an Amazonian environment. *Pesquisa Agropecuária Tropical*, v. 49, e54595, 2019.

MEDEIROS, J. C.; COOPER, M.; DALLA, R. J.; GRIMALDI, M.; COQUET, Y. Assessment of pedotransfer functions for estimating soil water retention curves for the Amazon region. *Revista Brasileira de Ciência do Solo*, v. 38, n. 3, p. 730-743, 2014.

NOBRE, P.; MALAGUTTI, M.; URBANO, D. F.; ALMEIDA, R. A. F.; GIAROLLA, E. Amazon deforestation and climate change in a coupled model simulation. *Journal of Climate*, v. 22, n. 21, p. 5686-5697, 2009.

NÓIA JÚNIOR, R. S.; SENTELHAS, P. S. Soybean-maize off-season double crop system in Brazil as affected by El Niño Southern Oscillation phases. *Agricultural Systems*, v. 173, n. 1, p. 254-267, 2019.

PAZ, J. O.; WOLI, P.; GARCIA, G. A.; HOOGENBOOM, G. Cotton yields as influenced by ENSO at different planting dates and spatial aggregation levels. *Agricultural Systems*, v. 111, n. 1, p. 45-52, 2012.

RAY, D. K.; GERBER, J. S.; MACDONALD, G. K.; WEST, P. C. Climate variation explains a third of global crop yield variability. *Nature Communications*, v. 6, e5989, 2015.

REIS, L.; SILVA, C. M. S.; BEZERRA, B.; MUTTI, P.; SPYRIDES, M. H.; SILVA, P.; MAGALHÃES, T.; FERREIRA, R.; RODRIGUES, D.; ANDRADE, L. Influence of climate variability on soybean yield in MATOPIBA, Brazil. *Atmosphere*, v. 11, e1130, 2020.

SENTELHAS, P. C.; BATTISTI, R.; CÂMARA, G. M. S.; FARIAS, J. R. B.; HAMPF, A. C.; NENDEL, C. The soybean yield gap in Brazil: magnitude, causes and possible solutions for sustainable production. *The Journal of Agricultural Science*, v. 153, n. 8, p. 1394-1411, 2015.

SHIMIZU, M. H.; AMBRIZZI, T.; LIEBMANN, B. Extreme precipitation events and their relationship with ENSO and MJO phases over northern South America. *International Journal of Climatology*, v. 37, n. 6, p. 2977-2989, 2017.

SILVA, E. H. F. M.; BOOTE, K. J.; HOOGENBOOM, G.; GONÇALVES, A. O.; ANDRADE, A. S.; MARIN, F. R. Performance of the CSM-CROPGRO-soybean in simulating soybean growth and development and the soil water balance for a tropical environment. *Agricultural Water Management*, v. 252, e106929, 2021.

SOUSA, A. M.; ROCHA, E. J. P.; VITORINO, M. I.; SOUZA, P. J. O.; BOTELHO, M. N. Variabilidade espaço-temporal da precipitação na Amazônia durante eventos ENOS. *Revista Brasileira de Geografia Física*, v. 8, n. 1, p. 13-24, 2015.

SOUZA, P. J. O. P.; FARIAS, J. R. B.; ABREU, J. P. M. M.; RIBEIRO, A.; ROCHA, E. J. P.; BOTELHO, M. N.; SOUSA, A. M. L. Simulation of soybean growth and yield under northeastern Amazon climatic conditions. *Pesquisa Agropecuária Brasileira*, v. 46, n. 6, p. 567-577, 2011.

UNITED STATES OF AMERICA (USA). National Weather Service. Climate Prediction Center. *Cold & warm episodes by season*. 2017. Available at: https://origin.cpc.ncep.noaa.gov/products/analysis_monitoring/ensostuff/ONI_v5.php. Access on: Mar. 27, 2022.

VILAYVONG, S.; BANTERNG, P.; PATANOTHAI, A.; PANNANGPETCH, K. CSM-CERES-rice model to determine management strategies for lowland rice production. *Scientia Agricola*, v. 72, n. 3, p. 229-236, 2015.

WALLACH, D.; MAKOWSKI, D.; JONES, J. W.; BRUN, F. Model evaluation. *In*: WALLACH, D.; MAKOWSKI, D.; JONES, J. W.; BRUN, F. *Working with dynamic crop models*: methods, tools, and examples for agriculture and environment. 2. ed. New York: Academic Press, 2014. p. 345-405.

WAONGO, M.; LAUX, P.; KUNSTMANN, H. Adaptation to climate change: the impacts of optimized planting dates on attainable maize yields under rainfed conditions in Burkina Faso. *Agricultural and Forest Meteorology*, v. 205, n. 1, p. 23-39, 2015.

WOLI, P.; ORTIZ, B. V.; JOHNSON, J.; HOOGENBOOM, G. El Niño: southern oscillation effects on winter wheat in the southeastern United States. *Agronomy Journal*, v. 107, n. 6, p. 2193-2204, 2015.

WOLI, P.; PAZ, J. O.; HOOGENBOOM, G.; GARCIA, G. A.; FRAISSE, C. W. The ENSO effect on peanut yield as influenced by planting date and soil type. *Agricultural Systems*, v. 121, n. 1, p. 1-8, 2013.